

An Optimal Framework for Constructing Lie-Algebra Generator Pools: Application to Variational Quantum Eigensolvers for Chemistry

Yaromir Viswanathan,¹ Olivier Adjoua,² César Feniou,^{2,1} Siwar Badreddine,^{1,*} and Jean-Philip Piquemal^{2,1,†}

¹*Qubit Pharmaceuticals, Advanced Research Department, 75014 Paris, France*

²*LCT, Sorbonne Université, UMR 7616 CNRS, 75005 Paris, France*

(Dated: December 2, 2025)

ABSTRACT

Lie Algebras are powerful mathematical structures used in physics to describe sets of operators and associated combinations. A central task is to identify a minimal set of generators from which the algebra can be constructed. The classical search for such generators has so far relied on greedy construction steps applied to an exponentially growing number of candidate operators, making it rapidly computationally intractable. We propose a general, polynomial-scaling and optimal strategy, based on Lie-Algebraic basic properties, to overcome this bottleneck. It allows for the efficient construction of these generators, also known as Minimal Complete Pools (MCPs), for a target Lie Algebra. As an immediate application, efficiently constructing user-defined MCPs that respect fermionic algebra is crucial in the context of adaptive Variational Quantum Eigensolver for quantum chemistry. Thus, we introduce MB-ADAPT-VQE, which incorporates optimally constructed MCPs into batched ADAPT-VQE to reduce quantum resources and improve convergence under strong correlation. These MCPs also unlock fixed-ansatz methods based on a Lie-algebraic structure such as the gradient-free NI-DUCC-VQE, enabling simulations surpassing prior MCP limits. The presented mathematical framework is general and applicable well beyond chemistry in fields including quantum error correction, quantum control, quantum machine learning, and more universally wherever compact Pauli basis are required.

I. INTRODUCTION

The evolution of quantum states is fundamentally described by unitary transformations that form a Lie group. The generators of these evolutions are elements of the corresponding Lie Algebra, which can be understood as the tangent space at the identity element of the Lie group when seen as a smooth manifold.

Lie Algebras are central in quantum computation, where any transformation can be realized as a sequence of unitary evolutions generated by operators from a specific Lie Algebra, typically $\mathfrak{su}(2^N)$ for a N -qubit system. A

key research area involves understanding the generation of these algebras from a minimal set of operators. For instance, when using a set of products of Pauli operators, it is known that a minimum of $2N + 1$ elements in this set is required to generate the full basis of $\mathfrak{su}(2^N)$ through nested commutation relations. The span of this basis is known as *Dynamical Lie Algebra (DLA)*, a term used in the context of quantum optimal control [1–7], and later adopted in quantum computing. Consequently, significant past work has aimed to investigate specific properties and applications of these bases. Broadly, these efforts can be categorized into two themes: foundational classification [2–7] and practical application in variational quantum algorithms [8–10].

One area of research has focused on fundamental properties and complete classification of these Lie Algebraic structures based on their generators. While some studies examined algebras within the context of specific physical models [2, 6, 7], a more general method maps the problem to a graph-theoretical setting [4], allowing for the classification of algebras generated by any arbitrary set of Pauli operators without physical constraints.

A related line of research focuses on the practical use of minimal generating sets for the target Lie Algebra. These sets, referred to as *Minimal Complete Pools (MCPs)*[11], offer a principled approach to the central challenge of constructing efficient unitary transformations in VQE [12]. This is particularly relevant for adaptive algorithms such as ADAPT-VQE [13]. Initial works by [8, 11, 14], explored the incorporation of complete pools with ADAPT-VQE where [8] later demonstrated that for molecular simulations, one needs *symmetry-adapted* pools that preserve the physical symmetries of the Hamiltonian to ensure convergence. To make this approach more practical, the authors in [9] developed an automated, greedy algorithm for constructing these symmetry-adapted pools and extended the framework to qubit-tapered systems. Building upon the construction of a complete symmetry-adapted generator set, [10] proposed a non-adaptive approach that effectively addresses the gradient measurement bottleneck of the ADAPT-VQE algorithm.

It is worth noting that each of these studies above involves a set of operators, known by several terms, including *operator pool* or *MCP* or *generating set* which serves to generate the basis of the Lie Algebra which spans the *DLA*. While the specific goals of these studies differ, they each seek to answer one of the following questions concerning this set:

* siwar.badreddine@qubit-pharmaceuticals.com

† jean-philip.piquemal@sorbonne-universite.fr

- What is the minimal size required to achieve universality or completeness?
- What are all the possible algebraic structures it can create?
- How can it be optimally selected or constructed to efficiently solve a specific problem?

The present work is focused on answering the third question: the optimal and efficient selection of these generators for a target Lie Algebra. As highlighted in some of the above studies [8–10, 15], the classical approach for generating and verifying a complete pool from an exponentially large number of candidate operators can be quite expensive. This work addresses this construction bottleneck by introducing a new theoretical framework to accelerate the process. We provide a general, efficient, scalable and provable method to construct and verify the completeness of the generator set (that incorporate desired properties) for a target Lie Algebra such as $\mathfrak{su}(2^N)$ or its relevant subalgebras. While our primary motivation is to apply this approach to quantum algorithms for quantum chemistry like ADAPT-VQE, the framework is general and suggests potential utility in other domains.

A simplified method for MCP construction:

In the context of quantum computation, we consider the generator set of Pauli operators. Our approach leverages the mapping between Pauli operators and the $\mathbb{F}_2^{2^N}$ vector space. This mapping provides a powerful framework to analyze the properties of a generator set without resorting to the computationally expensive, explicit construction of the DLAs basis. As highlighted in some of the mentioned studies, the conventional non-greedy approach is to iteratively compute nested commutators and check the dimension of the resulting algebra which scales poorly and is often intractable for even moderately sized systems. By translating the algebraic properties of the generators into this vector space representation, we reformulate the problem of verifying completeness of a given set of operators. We show that completeness is efficiently determined via the rank and congruence relations of a matrix of size $\mathcal{O}(N^2)$, derived from the generator’s vector space, as will be detailed in the subsequent sections.

MCPs for quantum chemistry: To set some context for the reader, in variational quantum chemistry, operator pools are used to construct efficiently an ansatz. These pools are complete, if their elements generate, under nested commutation relations, the basis of the Lie Algebra associated with the system’s Hamiltonian. In this case, there exists, in principle, a sequence of exponentials of these generators that can represent the exact ground state. Variational quantum algorithms are designed to construct and optimize precisely such an ansatz.

A Minimal Complete Pool (MCP) is a complete pool containing the smallest possible number of such

operators. For a generic n -qubit system, the theoretical minimum size for an MCP is $2n - 2$ operators [8, 9]. However, a critical challenge arises when applying these generic MCPs to quantum chemistry and the reason for this failure is the presence of symmetries. Molecular Hamiltonians have inherent symmetries that the ground state must obey. To solve this, a different kind of pools are required for quantum chemistry: a *symmetry-preserving MCP*. These pools are constructed specifically to respect the different properties of the molecular Hamiltonian and their size can be even smaller than $2n - 2$, a property we explore mathematically in this paper. While various methods exist to build such user-defined pools, our work presents a theoretical framework for constructing and applying them within variational quantum eigensolvers for chemistry.

Other applications: Based on a new theoretical framework, we present an efficient and scalable MCP construction algorithm with user-defined properties. As it will be detailed in Section IID, this method enables the exploration of larger molecular systems for quantum chemistry algorithms. This can also accelerate the preprocessing step in [2, 4, 6, 7] for building the minimal set that generates the basis of DLAs, which is then used to classify Lie Algebras. This classification has broad applications in quantum control [16], and in quantum machine learning[17, 18].

The remainder of this paper is organized as follows. Section IIA presents the main outcomes of our work, Section IIB then introduces the basic framework and key definitions. In Section IIC, we detail the main theorems involved in the efficient generation of MCPs. In Section IID, we provide two applications, within variational quantum eigensolvers, to validate our main results.

II. RESULTS

A. Summary of Main Lie Algebra Results

Here we give a brief summary of our main results: Let \mathcal{A} be the set of Pauli operators. Rather than analyzing the set \mathcal{A} , we construct an associated matrix, denoted by $\Gamma_{\mathcal{A}} \in \mathcal{M}_{|\mathcal{A}| \times |\mathcal{A}|}(\mathbb{F}_2)$ which contains sufficient information to determine if \mathcal{A} is a MCP. While a full description is provided in Section IIC, it is worth mentioning that the computation of this matrix is computationally cheap. The following is our main theoretical results.

- **Result 1** (MCP Congruence Theorem) A bracket-independent set \mathcal{A} is an MCP if its corresponding matrix, $\Gamma_{\mathcal{A}}$, is congruent to the matrix of a known MCP set. This provides a method for identifying MCPs via matrix transformations.
- **Result 2** (Characterizing \mathcal{A} via Matrix Rank) A

bracket-independent set \mathcal{A} is an MCP iff the rank of its matrix, $\text{rank}(\Gamma_{\mathcal{A}})$, equals the rank of a reference MCP matrix, $\text{rank}(\Gamma_{\mathcal{A}'})$. This reduces the problem of verifying an MCP to a simple rank evaluation.

The following table summarizes different approaches from the literature for verifying MCPs, alongside our proposed method. For more details on these existing methods, we refer the reader to Supplementary Material:

Approach	Completeness Guarantee	Computational Cost
Full Lie Algebra ^[8, 11] check	Yes (provable)	$\mathcal{O}(4^N)$ exponential
Product group ^[8] size+Inseparability	No (heuristic)	$\mathcal{O}(4^N)$ exponential
Greedy pool ^[9] construction	No (heuristic)	$\mathcal{O}(N^3)$ polynomial
Our work	Yes (provable)	$\mathcal{O}(N^3)$ polynomial

TABLE I

We summarize the main notations and nomenclature used throughout the paper in the following list.

Notations

Notation	Description
\mathfrak{g}	Lie Algebra
$\mathbf{A}, \mathbf{B}, \mathbf{C}$	Matrices
\mathcal{A}, \mathcal{B}	Sets
$ \mathcal{A} $	Cardinality of a set
$\mathcal{M}_{N \times N}(\mathbb{F}_2)$	Set of square $N \times N$ binary matrices
\otimes	Kronecker product (for arrays)
$[N]$	Set $\{i \in \mathbb{N} \mid 0 \leq i \leq N-1\}$
\circ	function composition

B. Preliminaries

In this section, we introduce the definitions required to define the $\Gamma_{\mathcal{A}}$ matrix, and subsequently to prove the results presented in Section II A.

Let $(\mathfrak{g}, [.,.])$ be a Lie Algebra equipped with a Lie bracket $[.,.] : \mathfrak{g} \times \mathfrak{g} \mapsto \mathfrak{g}$

Definition 1 (Adjoint map) The adjoint ad_{α} of an element $\alpha \in \mathfrak{g}$ is the endomorphism defined as

$$\begin{aligned} ad_{\alpha} : \mathfrak{g} &\mapsto \mathfrak{g} \\ \beta &\mapsto [\alpha, \beta] := \alpha\beta - \beta\alpha. \end{aligned} \quad (1)$$

Definition 2 (Bracket-closure) Given a set $\mathcal{A} = \{\alpha_j\}_{j \in [N]}$, $|\mathcal{A}| = N$, its bracket-closure is defined as

$$\langle \mathcal{A} \rangle_{[.,.]} := \bigcup_{n \in \mathbb{N}} \{ad_{\alpha_n} \circ \dots \circ ad_{\alpha_1}(\alpha_0) \in \mathfrak{g} \mid \{\alpha_j\}_{j \in [n]} \in \mathcal{A}^n\}. \quad (2)$$

This defines the set of all possible adjoint map sequences (or nested commutators) of elements in \mathcal{A} . By convention, the set in the union at index 0 is simply \mathcal{A} itself.

Definition 3 (Completeness) A Complete set for a Lie Algebra \mathfrak{g} is a subset $\mathcal{A} \in \mathfrak{g}$ such that

$$\langle \mathcal{A} \rangle_{Lie} := \text{span}_{\mathbb{F}}(\langle \mathcal{A} \rangle_{[.,.]}) = \mathfrak{g}. \quad (3)$$

This defines a set whose Lie-closure is \mathfrak{g} , or, equivalently, a set whose bracket-closure contains a \mathbb{F} -Hamel basis for \mathfrak{g} seen as a vector space over \mathbb{F} . In practice, it is common to see $\mathbb{F} := \mathbb{R}$. $\langle \mathcal{A} \rangle_{Lie}$ is also known as the DLA of dimension $|\langle \mathcal{A} \rangle_{[.,.]}|$.

Remark 4 We define a subset \mathcal{A} to be complete if it generates the Lie Algebra \mathfrak{g} . This condition is met if the linear combinations of all elements formed by successive applications of the Lie bracket to elements of \mathcal{A} generate the entire space \mathfrak{g} , such that

$$\mathfrak{g} \subseteq \langle \mathcal{A} \rangle_{Lie}. \quad (4)$$

The equality holds when the set \mathcal{A} is closed under the Lie Brackets. Since the scope of our analysis is restricted to subalgebras, we will adopt the condition in Definition 3 as the formal definition of completeness.

Definition 5 (Minimal Complete Pool (MCP)) A Minimal Complete Pool (MCP) of a given Lie Algebra is a complete set of minimal cardinality in the sense that any other complete set for the Lie Algebra will have an equal or larger cardinality.

In this paper, we will only consider Lie Algebras which have a natural basis consisting of Pauli strings. In particular, we will often consider $\mathfrak{su}(2^N)$, and its Lie-subalgebras. The Pauli strings can be defined as follows:

Definition 6 (Pauli Strings) Pauli matrices are a set of 2×2 complex matrices, defined as:

$$\begin{aligned} \mathbf{I} &:= \begin{pmatrix} 1 & 0 \\ 0 & 1 \end{pmatrix} & \mathbf{X} &:= \begin{pmatrix} 0 & 1 \\ 1 & 0 \end{pmatrix} \\ \mathbf{Y} &:= \begin{pmatrix} 0 & -i \\ i & 0 \end{pmatrix} & \mathbf{Z} &:= \begin{pmatrix} 1 & 0 \\ 0 & -1 \end{pmatrix}. \end{aligned} \quad (5)$$

A Pauli string (of length N) is a matrix of the form $\mathbf{P}_1 \otimes \dots \otimes \mathbf{P}_N$, $\mathbf{P}_i \in \{\mathbf{I}, \mathbf{X}, \mathbf{Y}, \mathbf{Z}\}$, $i \in [N]$. By convention, the Kronecker product symbol \otimes is suppressed, and Pauli strings are defined as a direct concatenation of

I, X, Y, Z , where X, Y, Z are short forms for the single-qubit Pauli matrices $\mathbf{X}, \mathbf{Y}, \mathbf{Z}$, respectively. In this paper, we define also a Pauli string by showing only the applied operators and their qubit indices. For example, for a 4-qubit system, the Pauli string $X_1Y_2Z_3 \equiv XYZI$.

Definition 7 (Pauli basis) *The set of matrices formed by N Kronecker products of any of the Paulis strings, defined as $\mathcal{P}_N = \{\mathbf{I}, \mathbf{X}, \mathbf{Y}, \mathbf{Z}\}^{\otimes N}$, is a basis of Hermitian $2^N \times 2^N$ matrices. We define $\mathcal{P}_N^* = \mathcal{P}_N \setminus \{\mathbf{I}^{\otimes N}\}$.*

Remark 8 *The set $i\mathcal{P}_N^*$ is a basis for $\mathfrak{su}(2^N)$ (set of skew-Hermitian matrices with vanishing trace).*

Hence, the Lie Algebras we will consider will always be endowed by the commutator as their Lie bracket.

Proposition 9 (Commutators) *Let $P_1, P_2 \in i\mathcal{P}_N^*$, we have*

$$[P_1, P_2] = \begin{cases} 0, \\ 2P_1P_2 = \pm 2P_3, \quad P_3 \in i\mathcal{P}_N^*. \end{cases} \quad (6)$$

Pauli strings can only either commute or anti-commute, and in the case that their commutator is nonzero, its result is a Pauli string multiplied by ± 2 .

The proof of this proposition is given in Supplementary Material.

C. Main theorems

We begin by defining the $\Gamma_{\mathcal{A}}$ matrices for a given set of Pauli strings, denoted as \mathcal{A} . These matrices are the adjacency matrices of the anti-commutation graphs introduced in [4].

Definition 10 (Anti-commuting pair-wise contraction [4]) *For a set of Pauli strings \mathcal{A} , a contraction of $\alpha \in \mathcal{A}$ onto $\beta \in \mathcal{A}$ is the process of removing β from \mathcal{A} and replacing it by $\beta\alpha = \frac{1}{2}[\beta, \alpha]$.*

It is easy to see that here the new set $\mathcal{A}' := (\mathcal{A} \setminus \{\beta\}) \cup \{\beta\alpha\}$ satisfies $\langle \mathcal{A}' \rangle_{[..]} = \langle \mathcal{A} \rangle_{[..]}$, however, $\Gamma_{\mathcal{A}'}$ will in general not be equal to $\Gamma_{\mathcal{A}}$. For clarity, we give an example in Figure 1.

It follows that $\Gamma_{\mathcal{A}}$ is defined as:

Definition 11 *Given a set of Pauli strings $\mathcal{A} := \{P_i\}_{i \in [|\mathcal{A}|]}$, we define $\Gamma_{\mathcal{A}} \in \mathcal{M}_{|\mathcal{A}| \times |\mathcal{A}|}(\mathbb{F}_2)$ as the binary matrix*

$$\Gamma_{\mathcal{A}}(i, j) := \begin{cases} 0, & [P_i, P_j] = 0 \\ 1, & \text{else.} \end{cases}$$

This matrix contains all commutation relations between elements in \mathcal{A} . Note that $\Gamma_{\mathcal{A}}$ matrices always have zero diagonal entries and are symmetric.

Remark 12 *We emphasize that from this point forward, any mention of an operation or property pertaining to a matrix over \mathbb{F}_2 will always be in the context of \mathbb{F}_2 -arithmetic, i.e., (mod 2).*

The main idea of [4] lies in reducing via contractions the graph whose edge relations are contained in the $\Gamma_{\mathcal{A}}$ matrix to a canonical graph corresponding to a set whose classification we know. By classification, we mean a means of telling exactly which Lie Algebra is generated via Lie-closure by a set of Pauli strings whose graph is canonical.

This idea can be extended to the $\Gamma_{\mathcal{A}}$ matrices through a linear algebraic framework. This perspective is more adapted to our final objective of efficiently and optimally constructing the MCPs for a given Lie Algebra.

For sake of clarity and brevity, we will present our results without proofs. Please refer to Supplementary Material for additional details and fully worked-out proofs.

As illustrated in Figure 1, the contraction of two Pauli strings P_i and P_j can be interpreted as applying a linear transformation over $\Gamma_{\mathcal{A}}$ matrices. This motivates the following proposition

Proposition 13 *Let \mathcal{A} be a set of Pauli strings and let $\Gamma_{\mathcal{A}}$ be the corresponding adjacency matrix as defined in 11. The contraction of two Pauli strings $P_i, P_j, i, j \in [|\mathcal{A}|]$, yields a new matrix, denoted as $\Gamma_{\mathcal{A}'}$, defined as:*

$$\Gamma_{\mathcal{A}'} = (\mathbf{e}_1 \dots (\mathbf{e}_i + \mathbf{e}_j) \dots \mathbf{e}_{|\mathcal{A}|})^\top \Gamma_{\mathcal{A}} (\mathbf{e}_1 \dots (\mathbf{e}_i + \mathbf{e}_j) \dots \mathbf{e}_{|\mathcal{A}|}), \quad (7)$$

where \mathbf{e}_i and \mathbf{e}_j are the i -th and j -th columns of $\Gamma_{\mathcal{A}}$.

Remark 14 *At the level of the $\Gamma_{\mathcal{A}}$ matrix, contraction of P_i onto P_j corresponds to adding (in \mathbb{F}_2) the i -th column onto the j -th column of the matrix, and similarly with the i -th and j -th rows. The order in which these two sums are executed can be interchanged. Both of these sums are elementary row operations whose elementary matrices are transposes of each other.*

It follows:

Proposition 15 *Let \mathcal{A} be a set of Pauli strings and let $\Gamma_{\mathcal{A}}$ be the corresponding adjacency matrix. There exists an invertible matrix denoted as $\mathbf{P} \in \mathcal{M}_{|\mathcal{A}| \times |\mathcal{A}|}(\mathbb{F}_2)$ such that $\Gamma_{\mathcal{A}}$ transforms to an equivalent matrix Γ_{equiv} through:*

$$\Gamma_{equiv} = \mathbf{P}^\top \Gamma_{\mathcal{A}} \mathbf{P}. \quad (8)$$

The proofs for Propositions 13 and 15 are detailed in Supplementary Material. The idea behind these propositions is that we can find a sequence of contractions, represented by a matrix \mathbf{P} , that transforms $\Gamma_{\mathcal{A}}$ into an equivalent matrix Γ_{equiv} with a known classification.

What is left to do now is to find "canonical" representatives for MCPs of different Lie Algebras. Although [4]

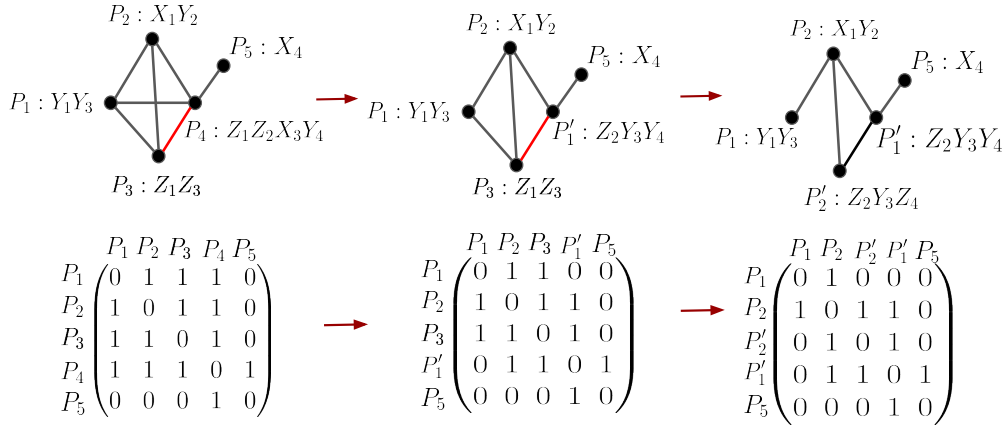


FIG. 1: We analyze the anti-commutation graph corresponding to the set of Pauli strings

$\mathcal{A} = \{Y_1Y_3, X_1Y_2, Z_1Z_3, Z_1Z_2X_3Y_4, X_4\}$, based on the work of [4]. As they demonstrate, such graphs can be simplified via vertex contraction. For example, contracting P_3 with P_4 produces a new string, $P'_1 = Z_2Y_3Y_4$, which simplifies the graph by reducing its connectivity. Our analysis will focus on the adjacency matrices of these graphs, hereafter denoted as $\Gamma_{\mathcal{A}}$.

proposes several families of graphs for their classification which we could transcribe into adjacency matrix form, we propose an alternate means for classification. The 2008 paper [19] presents the congruence classes for symmetric matrices over \mathbb{F}_2 . One such family of classes pertains to symmetric matrices with zero diagonal entries, which is precisely what are $\Gamma_{\mathcal{A}}$ matrices are. For such matrices, the congruence depends solely on the rank of the matrix. Furthermore, the possible ranks of such matrices can only be even. We use this complete classification of symmetric binary matrices of zero diagonal in order to classify MCPs via solely the rank of their corresponding $\Gamma_{\mathcal{A}}$ matrices.

Moving forward, before stating the main theorem, it is necessary to define the crucial concept of a bracket-independent set.

Definition 16 (*Bracket-independent set*) A set \mathcal{A} of Pauli strings is bracket-independent if no element in the set can be expressed as adjoint sequence of other elements. Formally, for each $P_j \in \mathcal{A}, j \in [|\mathcal{A}|]$, we have

$$P_j \notin \langle \mathcal{A} / \{P_j\} \rangle_{[\dots]}, \quad (9)$$

where $\langle \mathcal{A} \rangle_{[\dots]}$ is defined in Definition 2.

This leads to a fundamental property of MCPs, formalized below.

Proposition 17 Any MCP set is necessarily bracket-independent.

The corresponding proof is given in Supplementary Material.

We now have the necessary ingredients to present the main theorems 18 and 19 of this paper.

Theorem 18 (*MCP Congruence Theorem*) A set of Pauli strings \mathcal{A} is an MCP for a given Lie Algebra \mathfrak{g} if and only if there exists an invertible matrix $\mathbf{P} \in \mathcal{M}_{|\mathcal{A}| \times |\mathcal{A}|}(\mathbb{F}_2)$ such that

$$\mathbf{P}^\top \Gamma_{\mathcal{A}} \mathbf{P} = \Gamma_{\text{canonical-MCP}},$$

where $\Gamma_{\text{canonical-MCP}}$ is a canonical matrix for an MCP of \mathfrak{g} . Equivalently,

$$\Gamma_{\mathcal{A}} \sim \Gamma_{\text{canonical-MCP}},$$

where \sim denotes the congruence relation for matrices in $\mathcal{M}_{|\mathcal{A}| \times |\mathcal{A}|}(\mathbb{F}_2)$.

It follows

Theorem 19 (*Characterizing \mathcal{A} via Matrix Rank*) Let \mathcal{A} be a MCP for a given Lie Algebra \mathfrak{g} and let \mathcal{A}' be a set of bracket-independent Pauli strings. We have that:

$$\mathcal{A}' \text{ is MCP for } \mathfrak{g} \iff (\text{rank}(\Gamma_{\mathcal{A}}) = \text{rank}(\Gamma_{\mathcal{A}'})) \wedge (|\mathcal{A}| = |\mathcal{A}'|)$$

Corollary 20 Let \mathcal{A} be a MCP for a given Lie Algebra \mathfrak{g} and let \mathcal{A}' be a set of bracket-independent Pauli strings. We have that:

$$(\text{rank}(\Gamma_{\mathcal{A}}) = \text{rank}(\Gamma_{\mathcal{A}'})) \implies \mathcal{A}' \text{ is a CP for } \mathfrak{g}$$

The proofs of these theorems are given in Supplementary Material.

D. Outlook on Applications: Quantum Chemistry on Quantum Computers

The theoretical framework established in the preceding section enables a novel approach to the construction of MCPs.

As mentioned in the introduction, MCPs are fundamental building blocks for applications in variational quantum computing, such as the ones investigated in our numerical results. However, the practical utility of these applications is constrained by a significant precomputational bottleneck in the construction and verification of the MCP sets. For example, in the existing literature [8, 10], they mostly rely on building a *product group*, $G \subseteq i\mathcal{P}_N^*$ from a given set of Pauli strings, and in some case its associated DLAs basis. Although, they used physical symmetries to reduce the computational search space, the construction and verification of MCPs remains exponential with the number of qubits. These two applications have been restricted to systems of limited size, demonstrating results for up to $N = 12$ in [8] and $N = 14$ in [10].

Our work overcomes this critical limitation. Given a set of Pauli strings, our method analyzes their intrinsic algebraic properties, as described in Theorems 18 and 19, rather than the extensive properties of the resulting product group and DLAs. This yields a polynomial scaling.

In what follows we present a brief description of the applications employed:

ADAPT-VQE with MCPs: Here we focus on validating our MCP constructor for the Adaptive Derivative-Assembled Pseudo-Trotter Variational Quantum Eigensolver (ADAPT-VQE)[13]. ADAPT-VQE is a variational algorithm designed for approximating the ground state and the ground state energy of a given Hamiltonian $\mathbf{H} : \mathbb{R}^{2^n} \rightarrow \mathbb{R}^{2^n}$. The approximated ground state is a parametrized function that can be defined as:

$$|\Psi\rangle = \prod_{i=1}^M \exp(\theta_i U_i) |\Psi_0\rangle, \quad (10)$$

where $M \in \mathbb{N}^*$, and $\boldsymbol{\theta} = \{\theta_i\}_{i=1}^M$, $\theta_i \in \mathbb{R}$ is a list of parameters that completely characterize the state. $U_i, i \in [M]$ are unitary operators, can be defined also as excitation operators acting on a reference state $|\Psi_0\rangle$. This algorithm's distinct feature is its iterative approach to constructing this parametrized quantum state. At each iteration, the state is expanded by appending an exponentiated generator, which is carefully selected from a set of operator pools. The general workflow of this algorithm is described in Supplementary Material. There are many types of operator pools that can be used to construct the ADAPT-VQE ansatz, however one significant measurement overhead of ADAPT-VQE is the need to measure the energy gradient for every operator in the pre-defined operator pool which traditionally scales $\mathcal{O}(N^4)$

yielding a measurement cost of $\mathcal{O}(N^8)$. The work of [8], introduces a method to mitigate this cost by carefully constructing the operator pool, such that they use:

- MCPs as operator pools that scale linearly, $\mathcal{O}(N)$, which reduces the measurement overhead for molecular simulations to $\mathcal{O}(N^5)$.
- Symmetry-preserving MCPs where the elements of the set are chosen carefully to conserve all relevant symmetries and properties of the problem, as described in the following.
- An initial set with sufficient number of symmetry-preserving elements which will be a starting set for the MCP construction, in order to ensure that the algorithm can effectively begin its optimization from the initial Hartree-Fock state.

NI-DUCC-VQE approach: As introduced in [10], the NI-DUCC-VQE approach belongs to the class of "fixed-structure" ansatzes (initialized at the start of the VQE process that remain structurally unchanged, with only their parameters updated during optimization). The unitary operators U_i are derived from Pauli strings generated by MCPs, which scale linearly with the number of qubits. The expressivity of the NI-DUCC-VQE ansatz is ensured by employing a construction comprising k layers, such that:

$$|\Psi\rangle = \prod_{j=1}^k \left(\prod_{i=1}^M \exp(\theta_{ij} U_i) \right) |\Psi_0\rangle,$$

where $M = \mathcal{O}(N)$. Unlike iterative ansatz construction methods, this fixed-structure approach avoids the gradient evaluations in the operator selection step.

In our work, we combine these applications with our efficient MCP construction framework to process molecular systems of larger size.

Symmetries and properties of the pool: For molecular simulations with real-valued ansatz, the operator pool generators are restricted to odd Pauli strings (i.e odd number of Y operators in the string). The complete set of these generators forms the $\mathfrak{so}(2^N)$ Lie Algebra, see Supplementary Material. However, molecular Hamiltonians possess additional inherent symmetries, such as the conservation of particle number, total spin, spin projection, and spatial point-group symmetries, see Supplementary Material for more details. If the pool generators do not respect these symmetries, gradient-based algorithms like ADAPT-VQE can fail. This failure manifests as vanishing gradients, *symmetry roadblock* [8], preventing the algorithm from starting or converging.

In order to avoid this, the complete pool is typically constructed from an initial set of *starters*, which explains why we have adopted the term *user-defined* pools. These operators are specifically chosen to preserve all relevant

molecular symmetries. Using robust starters, selected via pre-screening criterion to identify the most significant contributing excitations, has been shown to dramatically improve convergence speed [10], see Figures 3 and 4.

It is worth mentioning that the set of operators that preserves all these molecular symmetries is not necessarily closed under the Lie brackets, i.e the commutator of two symmetric operators may produce a new operator that violates the desired symmetry (e.g. particle number, see Supplementary Material). Given that completeness requires the final pool to generate a mathematically closed Lie Algebra, the algebra generated from these starters will unavoidably expand to include operators that do not preserve all of the initial symmetries. We have therefore investigated which of these properties form a closed subalgebra. Our analysis indicates that the largest subalgebra that respects these constraints is defined by the two properties: the *odd string* requirement and the *even flip* property, the proof is detailed in Supplementary Material. We found numerically that the MCPs corresponding to this specific Lie subalgebra, which is a subalgebra of $\mathfrak{so}(2^N)$, have Γ_A matrices of rank $2N - 4$. This finding is currently numerical, as a formal proof and detailed characterization of this Lie subalgebra are beyond the scope of this work.

E. Numerical results

We validate our MCP construction algorithm by simulating a broad range of molecular systems. Our benchmarks include both iterative and fixed ansatz strategies. For the iterative case, we introduce a batched-ADAPT-VQE (MB-ADAPT-VQE) implementation based on our MCP, and for the fixed ansatz case, we apply the NI-DUCC-VQE approach [10] to larger molecules, demonstrating that our algorithm effectively eliminates the bottleneck previously associated with finding the MCP.

These methods are performed across systems ranging from 12 to 26 qubits, from weak to strongly correlated systems. The specific molecular benchmarks include: LiH ($R = 1.3\text{\AA}$, 12 qubits), the hydrogen chain H_6 ($R = 3.0\text{\AA}$, 12 qubits), H_8 ($R = 0.8\text{\AA}$, 16 qubits), and H_2O (26 qubits, geometry defined in Supplementary Material). All simulations were performed using our Hyperion statevector emulator [20]. We employed the minimal basis set (STO-3G) for most systems, while the 6-31G basis set was used specifically for the H_2O molecule. We assess ansatz performance across iterations using four metrics: energy accuracy, CNOT count, function evaluations (including the gradient measurements for ADAPT-VQE approaches), and the number of variational parameters.

MB-ADAPT-VQE (iterative ansatz): As a first practical test, we present a performance benchmark of a new ADAPT-VQE setup denoted MB-ADAPT-VQE. This composite strategy uses our newly introduced

MCPs (noted M) and adds to the ansatz a batch of k operators per iteration (where $k \in \{1, 5, 10, 20, 30\}$), an approach inspired by the so-called batched-ADAPT-VQE (denoted B), discussed in [9]. We employ the standard ADAPT-VQE with Qubit-Excitation-Based (QEB) pool [21] as a baseline for comparison with MB-ADAPT-VQE.

In Figure 2, we compare the convergence of absolute energy errors to the Full-CI (in Ha) versus function evaluations, number of CNOTs, and number of parameters. The red shaded area represents the chemical accuracy (Absolute Error $< 1.6 \times 10^{-3}$ Ha), the standard ADAPT-VQE (Blue line) uses a QEB pool, and the MB-ADAPT-VQE uses a complete pool generated via the construction strategy introduced earlier, which is verified to scale linearly with the number of qubits.

We first observe a consistent trend across all figures which is the sensitivity of the MB-ADAPT-VQE performance to the batch size k . We observe that increasing k generally accelerates the convergence. For instance, in the H_2O and H_8 systems, curves for $k = 20$ and $k = 30$ (red and purple lines) consistently outperform lower batch sizes ($k = 1$ or $k = 5$), converging faster to the chemical accuracy with significantly fewer function evaluations and comparable CNOT counts than the single-step approach. This suggests that estimating gradients after every individual operator may be unnecessarily costly, particularly for compact operator pools such as in MB-ADAPT-VQE.

For small systems (LiH, H_6), we observe that using a smaller operator pool is sufficient to reach the chemical accuracy. For **LiH** molecule, the standard ADAPT-VQE demonstrates a steady convergence, reaching the highest accuracy. In contrast, MB-ADAPT-VQE ($k = 20$) exhibits a superior initial convergence rate, crossing the chemical accuracy threshold significantly faster than the standard method. Lower k values ($k = 1, 5$) show plateau earlier, struggling to reach the required accuracy. In terms of number of CNOTs, standard ADAPT-VQE is more efficient, requiring fewer than 60 parameters and less than 600 CNOTs to reach high precision. While MB-ADAPT-VQE ($k = 20$) reaches chemical accuracy quickly in terms of optimization steps and gradient measurements, it incurs a higher cost in parameter count and gate depth (CNOTs) to achieve the same error compared to the standard ADAPT-VQE. For **H₆**, we observe that the MB-ADAPT-VQE ($k = 10$) demonstrates a dramatic reduction in measurement overhead, reaching chemical accuracy faster (in terms of function evaluations) than the standard ADAPT-VQE. The standard method shows a long tail requiring more evaluations to break the chemical accuracy barrier. MB-ADAPT-VQE ($k = 10$) achieves chemical accuracy with under 50 parameters and at approximately 200 CNOTs, whereas standard ADAPT-VQE requires nearly 150 parameters and significantly deeper circuits (> 1600 CNOTs) to reach the same threshold. For **H₈** molecule, the standard ADAPT-VQE regains its advantage. While MB-

ADAPT-VQE ($k = 20, 30$) performs respectably, the standard ADAPT-VQE maintains a steeper slope. Standard ADAPT-VQE reaches chemical accuracy with approximately 100 parameters and $\approx 1,500$ CNOTs. In contrast, the MB-ADAPT-VQE variants result in significantly heavier circuits (over 1,000 parameters and 8,000+ CNOTs) to reach similar error rates. For larger systems H_2O , the standard ADAPT-VQE demonstrates superior parameter efficiency in the early ansatz growth phase (< 500 parameters), while the MB-ADAPT-VQE strategy sacrifices more parameters and continue to reduce the error significantly further (reaching $\approx 2.5 \times 10^{-3}$ Ha) by using a larger ansatz.

Furthermore, the standard ADAPT-VQE shows initial slow convergence phase in terms of function evaluations, in contrast MB-ADAPT-VQE ($k = 10, k = 20, k = 30$) demonstrates a faster reduction in error. For example, to reach an error of 10^{-2} Ha, the MB-ADAPT-VQE ($k = 30$) requires approximately two orders of magnitude fewer function evaluations than the standard approach. In terms of number of CNOTs, the plot 2j reveals that a comparable accuracy as the standard ADAPT-VQE is achieved with less CNOTs gates required from MB-ADAPT-VQE ($k = 10, k = 20, k = 30$).

NI-DUCC-VQE (fixed ansatz): NI-DUCC-VQE has been previously introduced and already rigorously analyzed in [10], showing competitive performance against emerging fixed-ansatz methods such as COMPASS[22] and COMPACT[23]. However, prior applications were limited to systems of $N \leq 14$ qubits due to the computational bottleneck involved in constructing the Minimal Complete Pool (MCP). Here, we extend the applicability of NI-DUCC-VQE to larger systems and validate our construction strategy across three distinct cases: stretched H_6 , H_8 , and H_2O . The results, presented in Figure 3, collectively evaluate convergence efficiency with a focus on the number of layers denoted as k . For the strongly correlated system of stretched H_6 (12 qubits, $R = 3\text{\AA}$), the NI-DUCC-VQE algorithm shows robust convergence, rapidly reaching the chemical accuracy threshold. This performance is achieved with 295 parameters (1990 CNOTs) for $k = 5$ layers and 590 parameters (3980 CNOTs) for $k = 10$ layers. Having $k = 10$ layers, proves slightly more efficient, achieving lower final energy errors with a comparable number of function evaluations, a behavior observed in the H_8 system as well for ($k = 25$, 4350 parameters, 25800 CNOTs). Furthermore, for the 26-qubit H_2O system, the method achieves chemical accuracy in approximately 1,500 function evaluations with $k = 25$ (16725 parameters 99850 CNOTs). This can confirm, the method’s viability for larger-scale quantum simulations.

Pool choice and completeness: In Figures 4, 3a, and 3b, we evaluate the convergence behavior of MB-ADAPT-VQE and NI-DUCC, focusing specifically on the impact of pool completeness and the selection

strategy of the starters.

First, to assess the importance of the initial operator choice, we constructed pools using random selections of single and double excitations. We observe in Figure 3b that the NI-DUCC-VQE approach using these random pools (Green and Red lines) exhibits a rapid initial plateau at errors between 10^{-2} and 10^{-1} Ha, failing to reach the chemical accuracy threshold, a similar stagnation is observed with MB-ADAPT-VQE ($k = 30$) in Figure 4a. Second, we show in 3a that relying only on MCPs with a size of $2N - 4 = 20$ is insufficient. In Figure 3a, the "Only MCP" in the NI-DUCC-VQE approach ($k = 10$) approach (Red line) yields the poorest performance. Although the pool is formally complete, it was recognized early that adding a set of "starter" operators to MCPs in order to diversify search directions, helps avoid early plateaus and improves convergence. Conversely, using physically motivated but non-complete sets (Figures 3a, 4b, Orange line) results in a rapid initial descent that stagnates abruptly at the chemical accuracy border. Finally, in Figure 4a, we analyze a "small" complete pool strategy containing 60 operators (approximately twice the MCP size of 28) instead of 174, see Table II. While it converges more slowly than the standard MB-ADAPT-VQE ($k = 20$), it successfully breaks the chemical accuracy threshold with more iterations.

Benchmarking VQE approaches using MCPs: lessons learned. Using a smaller operator pool reduces the number of available update directions at each ADAPT-VQE step, which can lower the likelihood of selecting a high-impact operator at a given iteration. However, it also reduces the computational cost of the operator-selection stage, since ADAPT-VQE requires evaluating an energy gradient for every operator in the pool. MB-ADAPT-VQE is designed to balance this trade-off, reducing function evaluations while preserving the adaptive structure needed to mitigate barren plateaus. We benchmarked the approach on LiH and H_8 molecules, a strongly correlated system (stretched H_6), and a larger 26-qubit system (H_2O), with performance quantified by function evaluations (including gradient measurements), parameter count, and CNOT gate count. The corresponding pool sizes for MB-ADAPT-VQE and ADAPT-VQE using QEB pool, across these systems, are given in Table II.

Overall, the numerical results support the expected trends. Standard ADAPT-VQE tends to produce a slightly more compact ansatz, in terms of "operators-added-per-correlation-gained", for LiH, H_8 , and to a lesser extent H_2O . However, this compactness comes at the cost of a significantly larger number of function evaluations, driven by the size of the operator pool, which ultimately yields a much worse "function-evaluations-per-correlation-gained" ratio compared to MB-ADAPT-VQE.

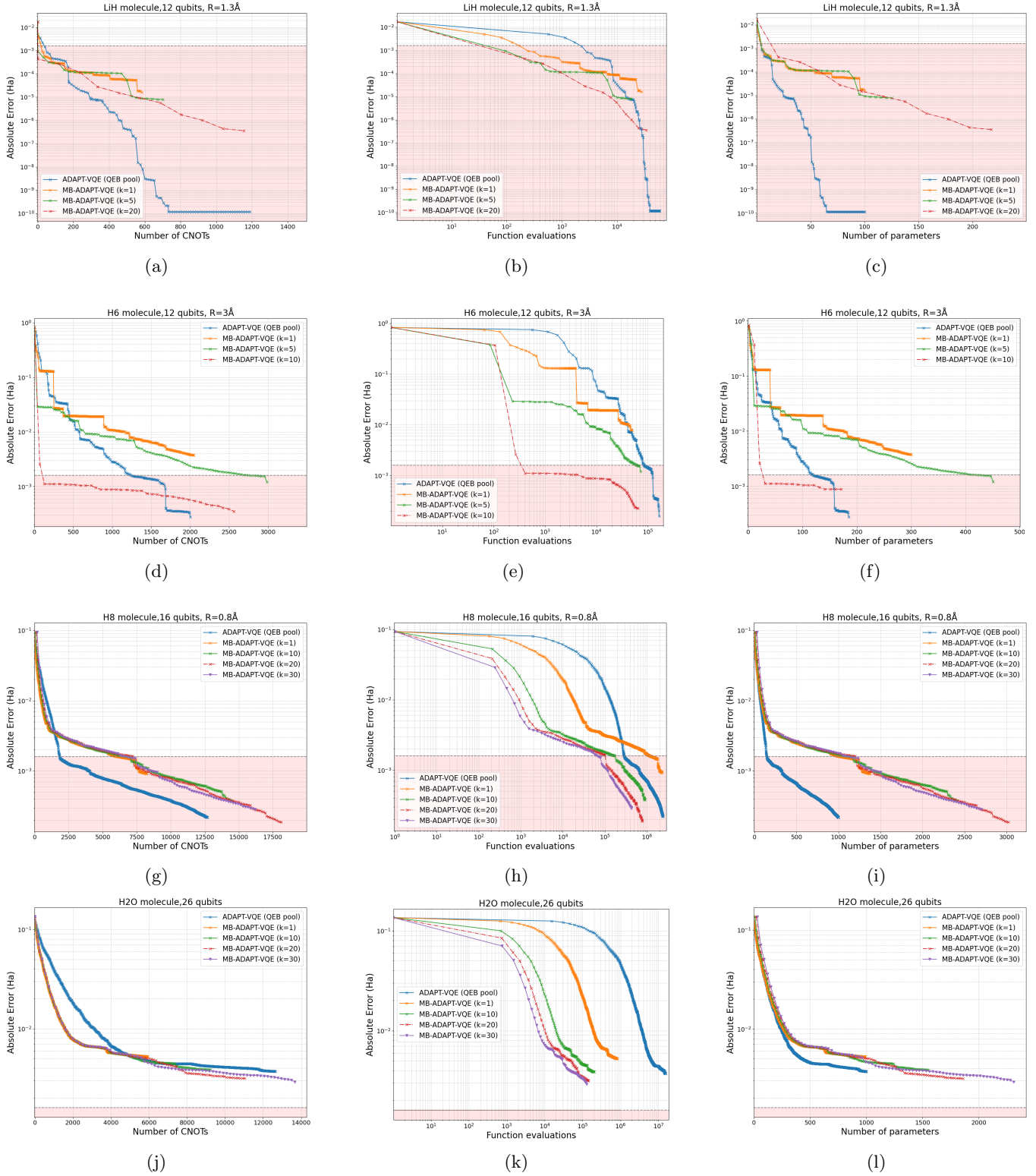


FIG. 2: Convergence plots for ADAPT-VQE and MB-ADAPT-VQE methods across various molecules: LiH ($R = 1.3\text{\AA}$, 12 qubits), the hydrogen chain H_6 ($R = 3.0\text{\AA}$, 12 qubits), H_8 ($R = 0.8\text{\AA}$, 16 qubits), and H_2O (26 qubits, geometry defined in Supplementary Material). The ADAPT-VQE method uses a QEB pool of size $\mathcal{O}(N^4)$. The composite MB-ADAPT-VQE method employs batched-ADAPT-VQE with efficient construction of MCPs of size $\mathcal{O}(N)$ for various values of k . Plots display energy errors versus CNOT count, function evaluations, and parameter count for different molecules.

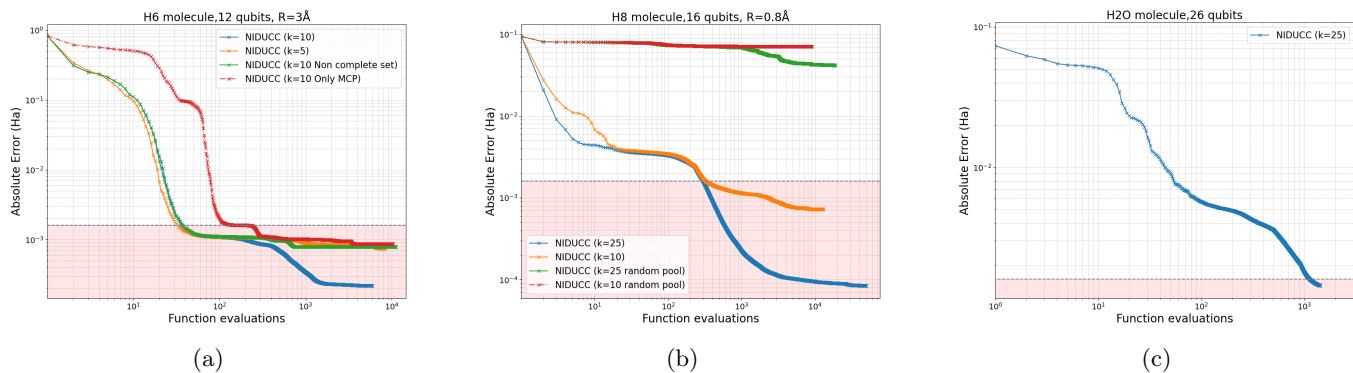


FIG. 3: Convergence plots for NI-DUCC-VQE method across various molecules using different pool operators: the hydrogen chain H_6 ($R = 3.0\text{\AA}$, 12 qubits), H_8 ($R = 0.8\text{\AA}$, 16 qubits), and H_2O (26 qubits, geometry defined in Supplementary Material). Plots display energy errors versus function evaluations.

Within MB-ADAPT-VQE, increasing the batch size consistently reduces the number of function evaluations required to reach a given accuracy, without degrading ansatz compactness. This establishes batching as an important strategy when working with reduced, but complete, operator pools.

The behavior also varies across correlation regimes. Standard ADAPT-VQE performs well for weakly correlated and moderately sized systems such as LiH and H_8 . In contrast, for strongly correlated systems such as stretched H_6 , MB-ADAPT-VQE with larger batches reaches chemical accuracy more efficiently. For the larger 26-qubit H_2O system, both approaches show signs of stagnation, likely due to vanishing gradients, an expected challenge in variational quantum algorithms as system size grows [24, 25] and one that may require additional techniques tailored to large, flat optimization landscapes.

Molecule	Size QEB pool	Size Complete pools
LiH	561	34
H_6	561	59
H_8	1940	174
H_2O	15275	667

TABLE II: Number of elements in the QEB pools vs the number of elements in complete pools used in our simulations.

We also benchmarked the performances of the NI-DUCC-VQE approach to extend its applicability to larger systems H_8 (16 qubits) and H_2O (26 qubits). We have noted that NI-DUCC-VQE exhibits exceptional convergence rates in terms of function evaluations. As shown in Figure 3, the method reaches chemical accuracy for H_2O in approximately 1500 evaluations. This is a dramatic reduction compared to typical variational runs, making NI-DUCC-VQE highly attractive to reduce the classical optimization overhead. The robustness of this method is further confirmed for H_8 and the strongly correlated stretched H_6 regime, where increasing layers to

$k = 10$ ensures convergence to chemical accuracy without being trapped in local minima. The trade-off for this classical speed is quantum circuit depth. For H_2O , the $k = 25$ NI-DUCC-VQE ansatz requires nearly 100,000 CNOTs. While feasible for state-vector emulators or ultimately for fault-tolerant hardware, this depth poses significant challenges for current NISQ devices.

Now, turning to the results in Figures 3a and 3b, an interesting observation emerges regarding the choice of operator pools. For random complete pools, the rapid stagnation (10^{-2} – 10^{-1} Ha) observed, shows that the pool requires operators that specifically target the physical system. Furthermore, we have observed that completeness alone does not guarantee efficient convergence and in contrast physically motivated but incomplete pools might fail and suffer from plateaus. Additionally, we have tried a "Small Complete Pool" strategy (Figure 4a) which seems to represent a viable middle ground: for example, by increasing the MCP of H_8 to 60 operators instead of having 174 operators, it reaches the chemical accuracy, but with slower convergence than the full MB-ADAPT-VQE pool. Ultimately, our study confirms that ansatz construction requires physics-informed operator pools, as random or purely mathematically complete sets lead to suboptimal convergence.

III. DISCUSSION

In this work, we proposed a general mathematical framework to verify the completeness of a user-defined pool of Pauli string operators with respect to a target Lie Algebra. This approach scales polynomially with the number of qubits where this complexity is determined by evaluating the rank of Γ_A binary matrices derived from the commutation relations of operators in the pool. Unlike known greedy strategies, we demonstrated that algebraic equivalence relationships allow the ranks of these matrices to provide definitive information regarding the completeness of the pool. While this is a general ap-

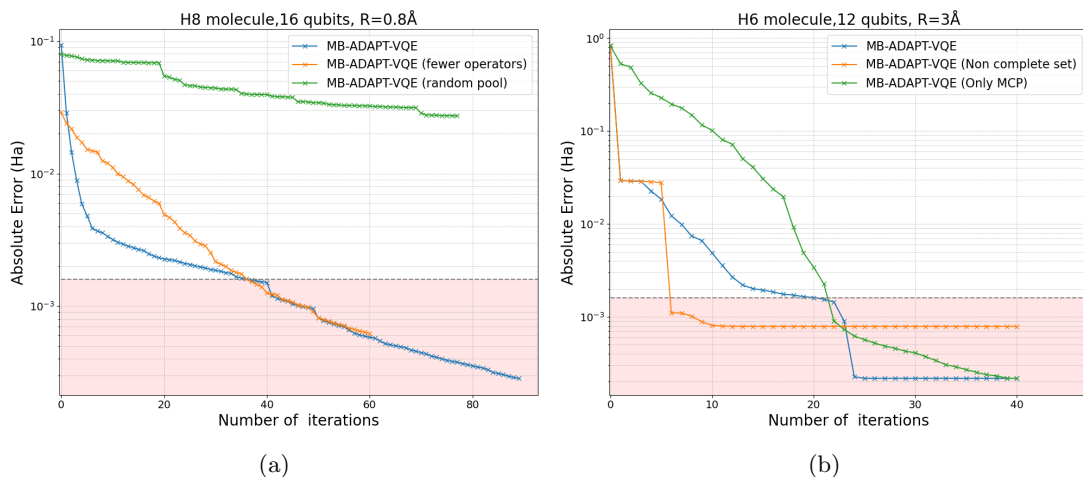


FIG. 4: Convergence plots for ADAPT-VQE and MB-ADAPT-VQE methods across H_6 ($R = 3.0\text{\AA}$, 12 qubits), and H_8 ($R = 0.8\text{\AA}$, 16 qubits) using different pool operators. Plots display energy errors versus number of iterations.

proach applied to a variety of contexts, we specifically validated it within variational quantum algorithms for quantum chemistry. Therefore, using our construction strategy, we built symmetry-preserving MCPs aligned with the physical symmetries of a target problem. Because MCPs yield an operator pool that scales as $\mathcal{O}(N)$ rather than the usual $\mathcal{O}(N^4)$, adaptive VQE algorithms benefit from much lower gradient-evaluation overhead. With MCPs coupled to batched ADAPT, we achieve faster convergence in challenging regimes with respect to the number of energy evaluations, while also enabling the scalability gradient-free NI-DUCC-VQE ansatz previously limited by classical MCP construction cost. It is worth noting that these efforts align with the broad interest in making operator selection more efficient in adaptive variational methods, as seen in recent approaches [26–29]. Overall, this new theoretical framework allows efficient classical construction of MCPs for a given Lie Algebra. We validated their use in the context of variational quantum algorithms, overcoming limitations of earlier approaches. Because minimal Pauli generator structures are foundational in stabilizer codes [30–32], the efficient MCP construction introduced here may support application in quantum error correction, and more generally wherever compact Pauli basis are useful, e.g. in quantum control [33], quantum machine learning and Hamiltonian simulation [34], and might as well contribute to Lie Algebras classifications. Concrete avenues for future investigations include:

- **Sub-Lie Algebra characterization:** we aim to further characterize the sub-Lie Algebras obtained from symmetry-preserving pools. While numerical ranks found for these pools are $2N - 4$, the theoretical properties of the sub-algebra generated is still under investigation. Furthermore, the theoretical significance of the ranks of these $\Gamma_{\mathcal{A}}$ matrices, and how they can be related to the DLAs, is currently

under investigation.

- **Basis selection:** Given the impact of the choice of the operator pool on the convergence of variational algorithms for quantum chemistry, determining the best basis for building MCPs, the number of starters, and the optimal algorithm for their selection remains an open question. Possible way forward include cheap energy sorting heuristics as introduced in [14].
- **Compactification techniques:** We note that MB-ADAPT-VQE lacks a very compact representation that can likely be improved at a cheap cost using overlap-driven compactification techniques as introduced in [35, 36].

IV. METHODS

Efficient binary representation of Pauli strings

As mentioned previously in this work, it is extremely computationally advantageous to map N -qubit Pauli strings to \mathbb{F}_2^{2N} . Multiple such mappings exist, but one mapping in particular is slightly preferred as it allows for some distinct bits to be contiguous in memory. It is known that $Y = iXZ$, therefore, we may always decompose a given Pauli string using only X and Z components by considering it a product of an X part and a Z part.

Example 1 Consider $P = IXYZ$. We may write it as $P = e^{i\theta}(IXXI)(IIZZ) =: e^{i\theta}P_X P_Z$. Recall that following convention, we suppress the Kronecker product between I, X, Y, Z terms in a Pauli string, and we suppress the matrix product between P_X and P_Z . Note that we will often forgo the $e^{i\theta}$ term, as this will always be either ± 1 or $\pm i$ and will always be unique. This term simply counterbalances the $\pm i$ terms which arise when you multiply

X and Z terms together to form a Y term. We will drop this term in future references to this decomposition.

Definition 2 We introduce the map

$$\phi : \mathcal{P}_N \longrightarrow \mathbb{F}_2^{2N}.$$

Given a decomposition $P = P_X P_Z$, we create one array of length N for the P_X part, and one for the P_Z part. Each array simply houses a 1 at the indices where P_X (resp. P_Z) houses a X (resp. Z) term, and a 0 wherever it houses the identity.

Keeping the previous example 1, we obtain that $\phi(P) = [0110\ 0011]$.

Remark 3 This mapping convention requires that the first N entries of the binary string correspond to the P_X part, and that the latter N entries correspond to the P_Z part. An alternate mapping proposes that instead of mapping P to $[x_1 \cdots x_n\ z_1 \cdots z_n]$ where the x_i are the bits corresponding to P_X and the z_i are the bits corresponding to P_Z , we map P to $[x_1 z_1 x_2 z_2 \cdots x_n z_n]$. In practice, it is advantageous to have the binary representations of P_X and P_Z contiguous in memory. The following proposition is an example of why this is true.

Proposition 4 Consider two Pauli strings $P = P_X P_Z$ and $P' = P'_X P'_Z$ of the same length. As an abuse of notation, we note $\phi(P) = [\phi(P_X)\ \phi(P_Z)]$. Then,

$$\phi(P_X)^T \phi(P'_Z) + \phi(P_Z)^T \phi(P'_X) \pmod{2}$$

is a quantity which is equal to 0 when P, P' commute, and 1 if not.

Remark 5 The example above is one of many that show how the ϕ map translates the properties and operations of Pauli strings into linear-algebraic operations, many of which, from a computational point of view, benefit from having the $\phi(P_X)$ and $\phi(P_Z)$ parts contiguous in memory.

Operator pool construction

We give in Figure 5, an illustrated scheme on different steps towards a user-defined complete pool. As mentioned above, for our user-defined pool, which targets molecular Hamiltonians, the process begins with an initial set of *starters*. These starters must preserve specific symmetries and properties (see Supplementary Material), such as odd strings, even flip, particle number, and spin. These starters can be selected in several ways: random selection from subgroups $G \subseteq i\mathcal{P}_N^*$ that preserve desired symmetries, random selection from UCCSD operator pool (accounting only for single and double excitations) [9, 10], or using the UCCSD pool combined with prescreening techniques to select the most significant contributors to energy convergence [10]. Once the starters are chosen, the complete pool is built iteratively.

We add new elements that preserve the required symmetries, provided they meet two conditions: first, that the element does not already exist in the set, and second, that it is bracket-independent, see Definition 16. The latter is confirmed either by checking the linear independence, as done in [9], or by verifying that it cannot be written as an adjoint sequence. We then evaluate the rank of $\Gamma_{\mathcal{A}} \in \mathbb{R}^{|\mathcal{A}| \times |\mathcal{A}|}$ for the updated set \mathcal{A} . The algorithm terminates if the rank is $\text{rank}(\Gamma_{\mathcal{A}}) = 2N - 4$. It is worth noting that while our code returns exactly a minimal complete pool, an MCP is often insufficient for convergence. Therefore, we typically add more starters and work with larger, Complete Pools (CP) in our simulations. Finally these CPs are used to construct the ansatz, either using fixed (NI-VQE) or iterative methods such as ADAPT-VQE or its variants (e.g batched ADAPT [9]).

Computational details

All simulations mentioned above ran onto accelerated computing nodes equipped with NVIDIA A100 and H100 GPU cards. Except for H_2O , all other molecules require a single 40GB card from a DGX-A100 machine to host the simulations; while H_2O required 8 H100 with 80GB each, due to the storage requirements of the Hamiltonian matrix, i.e. approximately 472 Gigabytes in its Compressed Sparse Row (CSR) format. This latter molecule simulation naturally operated in parallel, and was performed on the Jean Zay supercomputer (IDRIS) at GENCI, whose recent partition is equipped with a set of 4 interconnected H100 Cards per node, each node exchanging data through a NDR InfiniBand 400GB network.

ACKNOWLEDGMENTS

GPU computations have been performed at GENCI (IDRIS, Orsay, France) on grant no A0190712052.

FUNDING

This work has received funding from the European Research Council (ERC) under the European Union’s Horizon 2020 research and innovation program (grant agreement No 810367), project EMC2 (JPP). Support from the PEPR EPIQ - Quantum Software (ANR-22-PETQ-0007, JPP) and HQI (JPP) programs is acknowledged.

COMPETING INTERESTS

JPP is shareholder and co-founder of Qubit Pharmaceuticals. The remaining authors declare no other competing interests.

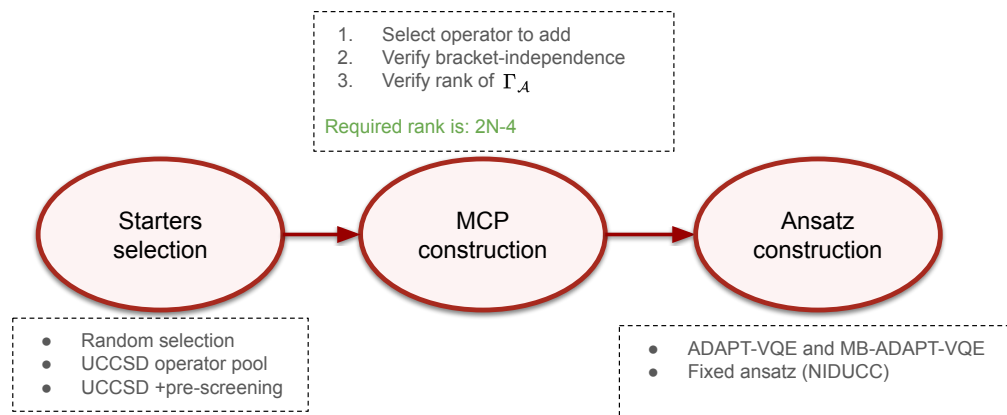


FIG. 5: Schematic of necessary steps towards a user-defined operator pool

- [1] F. Albertini and D. D'Alessandro. Notions of controllability for quantum mechanical systems. In *Proceedings of the 40th IEEE Conference on Decision and Control (Cat. No. 01CH37228)*, volume 2 of *CDC-01*, page 1589–1594. IEEE, 2001.
- [2] Roeland Wiersema, Efehan Kökcü, Alexander F. Kemper, and Bojko N. Bakalov. Classification of dynamical lie algebras of 2-local spin systems on linear, circular and fully connected topologies. *npj Quantum Information*, 10(1), November 2024.
- [3] Matthew L. Goh, Martin Larocca, Lukasz Cincio, M. Cerezo, and Frédéric Sauvage. Lie-algebraic classical simulations for quantum computing. *Physical Review Research*, 7(3), September 2025.
- [4] Gerard Aguilar, Simon Cichy, Jens Eisert, and Lennart Bittel. Full classification of pauli lie algebras. *ArXiv:2408.00081* <https://arxiv.org/abs/2408.00081>, 2024.
- [5] Isaac D. Smith, Maxime Cautrès, David T. Stephen, and Hendrik Poulsen Nautrup. Optimally generating $\mathfrak{su}(2^N)$ using pauli strings. *Physical Review Letters*, 134(20), May 2025.
- [6] Efehan Kökcü, Roeland Wiersema, Alexander F. Kemper, and Bojko N. Bakalov. Classification of dynamical lie algebras generated by spin interactions on undirected graphs, 2024.
- [7] Sujay Kazi, Martín Larocca, Marco Farinati, Patrick J. Coles, M. Cerezo, and Robert Zeier. Analyzing the quantum approximate optimization algorithm: Ansätze, symmetries, and lie algebras. *PRX Quantum*, 6(4), November 2025.
- [8] V. O. Shkolnikov, Nicholas J. Mayhall, Sophia E. Economou, and Edwin Barnes. Avoiding symmetry roadblocks and minimizing the measurement overhead of adaptive variational quantum eigensolvers. *Quantum*, 7:1040, June 2023.
- [9] Mariia D. Sapova and Aleksey K. Fedorov. Variational quantum eigensolver techniques for simulating carbon monoxide oxidation. *Communications Physics*, 5(1), August 2022.
- [10] Mohammad Haidar, Olivier Adjoua, Siwar Badreddine, Alberto Peruzzo, and Jean-Philip Piquemal. Non-iterative disentangled unitary coupled-cluster based on lie-algebraic structure. *Quantum Science and Technology*, 10(2):025031, February 2025.
- [11] Ho Lun Tang, V.O. Shkolnikov, George S. Barron, Harper R. Grimsley, Nicholas J. Mayhall, Edwin Barnes, and Sophia E. Economou. Qubit-adapt-vqe: An adaptive algorithm for constructing hardware-efficient ansätze on a quantum processor. *PRX Quantum*, 2(2), April 2021.
- [12] Artur F Izmaylov, Manuel Díaz-Tinoco, and Robert A Lang. On the order problem in construction of unitary operators for the variational quantum eigensolver. *Physical Chemistry Chemical Physics*, 22(23):12980–12986, 2020.
- [13] Harper R. Grimsley, Sophia E. Economou, Edwin Barnes, and Nicholas J. Mayhall. An adaptive variational algorithm for exact molecular simulations on a quantum computer. *Nature Communications*, 10(1), July 2019.
- [14] César Feniou, Muhammad Hassan, Baptiste Claudon, Axel Courtat, Olivier Adjoua, Yvon Maday, and Jean-Philip Piquemal. Greedy gradient-free adaptive variational quantum algorithms on a noisy intermediate scale quantum computer. *Scientific Reports*, 15(1):1–18, 2025.
- [15] Yutaro Iiyama. Fast numerical generation of lie closure, 2025.
- [16] S. G. Schirmer, H. Fu, and A. I. Solomon. Complete controllability of quantum systems. *Physical Review A*, 63(6), May 2001.
- [17] Maria Schuld, Ilya Sinayskiy, and Francesco Petruccione. An introduction to quantum machine learning. *Contemporary Physics*, 56(2):172–185, October 2014.
- [18] Johannes Jakob Meyer, Marian Mularski, Elies Gil-Fuster, Antonio Anna Mele, Francesco Arzani, Alissa Wilms, and Jens Eisert. Exploiting symmetry in variational quantum machine learning. *PRX Quantum*, 4(1), March 2023.
- [19] Yong-Hyuk Kim and Keomkyo Seo. Two congruence classes for symmetric binary matrices over \mathbb{F}_2 . *WSEAS Transactions on Mathematics*, 7, 01 2008.
- [20] Sorbonne Université Olivier Adjoua et al. and Qubit Pharmaceuticals. The hyperion emulator, 2025.
- [21] Yordan S. Yordanov, V. Armaos, Crispin H. W. Barnes, and David R. M. Arvidsson-Shukur. Qubit-excitation-based adaptive variational quantum eigensolver. *Communications Physics*, 4(1), October 2021.
- [22] Dibyendu Mondal, Dipanjali Halder, Sonaldeep Halder, and Rahul Maitra. Development of a compactansatz via operator commutativity screening: Digital quantum simulation of molecular systems. *The Journal of Chemical Physics*, 159(1), July 2023.
- [23] Dipanjali Halder, Dibyendu Mondal, and Rahul Maitra. Noise-independent route toward the genesis of a compact ansatz for molecular energetics: A dynamic approach. *The Journal of Chemical Physics*, 160(12), March 2024.
- [24] Jarrod R McClean, Sergio Boixo, Vadim N Smelyanskiy, Ryan Babbush, and Hartmut Neven. Barren plateaus in quantum neural network training landscapes. *Nature Communications*, 9(1):4812, 2018.
- [25] Martín Larocca, Supanut Thanasilp, Samson Wang, Kunal Sharma, Jacob Biamonte, Patrick J. Coles, Lukasz Cincio, Jarrod R. McClean, Zoë Holmes, and M. Cerezo. Barren plateaus in variational quantum computing. *Nature Reviews Physics*, 7(4):174–189, March 2025.
- [26] Rick Huang and Artur F Izmaylov. Quantum gambling: Best-arm strategies for generator selection in adaptive variational algorithms. *arXiv preprint arXiv:2509.14917*, 2025.
- [27] Panagiotis G Anastasiou, Nicholas J Mayhall, Edwin Barnes, and Sophia E Economou. How to really measure operator gradients in adapt-vqe. *arXiv preprint arXiv:2306.03227*, 2023.
- [28] Jie Liu, Zhenyu Li, and Jinlong Yang. An efficient adaptive variational quantum solver of the schrödinger equation based on reduced density matrices. *The Journal of chemical physics*, 154(24), 2021.
- [29] Zhihao Lan and WanZhen Liang. Amplitude reordering accelerates the adaptive variational quantum eigensolver algorithms. *Journal of Chemical Theory and Computation*, 18(9):5267–5275, 2022.
- [30] Daniel Gottesman. Stabilizer codes and quantum error correction. *arXiv preprint arXiv:quant-ph/9705052*, 1997.

- [31] M. A. Nielsen and I. L. Chuang. *Quantum Computation and Quantum Information*. Cambridge University Press, 2000.
- [32] Guillaume Dauphinais, David W Kribs, and Michael Vasmer. Stabilizer formalism for operator algebra quantum error correction. *Quantum*, 8:1261, 2024.
- [33] Jin-Fang Li, Zi-Xuan Xin, Jie-Ru Hu, and Dong-Shan He. Quantum optimal control for pauli operators based on spin-1/2 system. *International Journal of Theoretical Physics*, 61(12):268, 2022.
- [34] Smik Patel, Tzu-Ching Yen, and Artur F Izmaylov. Extension of exactly-solvable hamiltonians using symmetries of lie algebras. *The Journal of Physical Chemistry A*, 128(20):4150–4159, 2024.
- [35] César Feniou, Muhammad Hassan, Diata Traoré, Emmanuel Giner, Yvon Maday, and Jean-Philip Piquemal. Overlap-adapt-vqe: practical quantum chemistry on quantum computers via overlap-guided compact ansätze. *Communications Physics*, 6(1):192, 2023.
- [36] César Feniou, Olivier Adjoua, Baptiste Claudon, Julien Zylberman, Emmanuel Giner, and Jean-Philip Piquemal. Sparse quantum state preparation for strongly correlated systems. *The Journal of Physical Chemistry Letters*, 15:3197–3205, 2024. PMID: 38483286.